⌘ *Author's Choice*

THE JOURNAL OF BIOLOGICAL CHEMISTRY VOL. 287, NO. 4, pp. 2308–2315, January 20, 2012

Photoaffinity Labeling of High Affinity Nicotinic Acid Adenine Dinucleotide Phosphate (NAADP)-Binding Proteins in Sea Urchin Egg*[S]◆

Received for publication, October 10, 2011, and in revised form, November 16, 2011 Published, JBC Papers in Press, November 23, 2011, DOI 10.1074/jbc.M111.306563

Timothy F. Walseth[‡1], Yaping Lin-Moshier[‡2], Pooja Jain[§], Margarida Ruas[¶], John Parrington[¶], Antony Galione[¶], Jonathan S. Marchant[‡], and James T. Slama[§]

From the [‡]Department of Pharmacology, University of Minnesota Medical School, Minneapolis, Minnesota 55455, the [§]Department of Medicinal and Biological Chemistry, University of Toledo, Toledo, Ohio 43614, and the [¶]Department of Pharmacology, University of Oxford, Mansfield Road, Oxford OX1 3QT, United Kingdom

Background: Nicotinic acid adenine dinucleotide phosphate (NAADP) regulates calcium release from internal acidic stores via two-pore channels (TPCs).
Results: A novel photosensitive probe (5-azido-NAADP) identified high affinity NAADP binding sites that interact with, but are distinct from, TPCs.
Conclusion: High affinity NAADP-binding proteins complex with TPCs.
Significance: This work provides new mechanistic insights into how NAADP regulates calcium release via TPCs.

Nicotinic acid adenine dinucleotide phosphate (NAADP) is a messenger that regulates calcium release from intracellular acidic stores. Recent studies have identified two-pore channels (TPCs) as endolysosomal channels that are regulated by NAADP; however, the nature of the NAADP receptor binding site is unknown. To further study NAADP binding sites, we have synthesized and characterized [^{32}P-5-azido]nicotinic acid adenine dinucleotide phosphate ([^{32}P-5N$_3$]NAADP) as a photoaffinity probe. Photolysis of sea urchin egg homogenates preincubated with [^{32}P-5N$_3$]NAADP resulted in specific labeling of 45-, 40-, and 30-kDa proteins, which was prevented by inclusion of nanomolar concentrations of unlabeled NAADP or 5N$_3$-NAADP, but not by micromolar concentrations of structurally related nucleotides such as NAD, nicotinic acid adenine dinucleotide, nicotinamide mononucleotide, nicotinic acid, or nicotinamide. [^{32}P-5N$_3$]NAADP binding was saturable and displayed high affinity (K_d ~10 nM) in both binding and photolabeling experiments. [^{32}P-5N$_3$]NAADP photolabeling was irreversible in a high K$^+$ buffer, a hallmark feature of NAADP binding in the egg system. The proteins photolabeled by [^{32}P-5N$_3$]NAADP have molecular masses smaller than the sea urchin TPCs, and antibodies to TPCs do not detect any immunoreactivity that comigrates with either the 45-kDa or the 40-kDa photolabeled proteins. Interestingly, antibodies to TPC1 and TPC3 were able to immunoprecipitate a small fraction of the 45- and 40-kDa photolabeled proteins, suggesting that these proteins associate with TPCs. These data suggest that high affinity NAADP binding sites are distinct from TPCs.

NAADP[3] is a naturally occurring nucleotide that has been shown to be involved in the release of intracellular calcium from acidic intracellular stores in a wide variety of cell types (1, 2). Mounting evidence suggests that NAADP may function as a trigger to initiate a calcium signal that is then amplified by other calcium release mechanisms (3). However, a fundamental question that remains unanswered is the identity of the NAADP receptor. Recently, the two-pore channel (TPC) family of endolysosomal proteins was shown to be regulated by NAADP (4–6). Multiple approaches, including molecular manipulation of TPC levels by overexpression (4–7) or knockdown (4, 5), as well as electrophysiological analyses (8–11), all support the role of TPCs as NAADP-sensitive Ca^{2+} channels. However, whether TPCs directly interact with NAADP remains an important unresolved issue. Notably, overexpression of mammalian TPC2 modestly increased [^{32}P]NAADP binding activity, but the increase in binding was much lower than the increase in TPC2 mRNA levels (3-fold *versus* ~250-fold) (4). Although [^{32}P]NAADP binding activity was also found in immunoprecipitation studies using antibodies to sea urchin TPCs (12), very little is known regarding the interaction between NAADP and TPCs.

Photoaffinity labeling is a powerful technique for identifying and characterizing receptors and binding sites for appropriately labeled ligands (13, 14). In this study, we have synthesized and characterized [^{32}P-5N$_3$]NAADP as a photoaffinity probe for NAADP binding sites. Previous studies with 5N$_3$-NAADP indicated that this NAADP analog was able to release calcium and complete with NAADP for high affinity binding sites (15).

* This work was supported, in whole or in part, by National Institutes of Health Grant GM088790 (to J. S. M.). This work was also supported by University of Minnesota Academic Health Center Seed Grant 2101.95 (to T. F. W.) and a Wellcome Trust Programme Grant (to A. G. and J. P.).
◆ This article was selected as a Paper of the Week.
⌘ *Author's Choice*—Final version full access.
[S] This article contains supplemental Figs. 1S and 2S.
[1] To whom correspondence should be addressed. Tel.: 612-625-2627; Fax: 612-625-8408; E-mail: walse001@umn.edu.
[2] Supported by a doctoral dissertation fellowship from the University of Minnesota Graduate School.

[3] The abbreviations used are: NAADP, nicotinic acid adenine dinucleotide phosphate; 5N$_3$-NAADP, 5-azido-NAADP; NAAD, nicotinic acid adenine dinucleotide; TPC, two-pore channels.

The sea urchin egg system was chosen for this study because high affinity binding in this system has been well characterized and is considered the "gold standard" for studying NAADP function. [^{32}P-5N$_3$]NAADP photolabeling was found to specifically label 45-, 40-, and 30-kDa proteins in *Strongylocentrotus purpuratus* homogenates. The properties of the photolabeled proteins matched NAADP binding in terms of selectivity and irreversibility in high potassium. Antibodies to TPCs did not recognize the 45- and 40-kDa proteins. Interestingly, the 45- and 40-kDa photolabeled proteins were found in immunoprecipitates using TPC1 and TPC3 antibodies. Overall, the data suggest that the [^{32}P-5N$_3$]NAADP photoaffinity probe detects high affinity NAADP binding sites and that these proteins are distinct from, but interact with, TPCs. The [^{32}P-5N$_3$]NAADP photoprobe should prove to be a valuable tool in the identification of NAADP-binding proteins and elucidation of the mechanism by which NAADP regulates mobilization of intracellular calcium.

EXPERIMENTAL PROCEDURES

Materials—HEPES, CHAPS, potassium gluconate, *N*-methylglucamine, NAD, NAAD, NADP, nicotinamide mononucleotide, nicotinic acid, nicotinamide, ATP, and DTT were from Sigma. Laemmli sample buffer, 12.5% Criterion acrylamide gels, and AG MP-1 resin were obtained from Bio-Rad. SimplyBlue SafeStain was obtained from Invitrogen. Recombinant human NAD kinase was purchased from Alexis Biochemicals. Complete protease inhibitor tablets were from Roche Applied Science. ECL reagents were obtained from GE Healthcare. [^{32}P]NAD (800 Ci/mmol) was from PerkinElmer Life Sciences. NAADP, 5N$_3$-NAADP, and 5N$_3$-nicotinic acid were prepared as described previously (15).

Sea Urchin Egg Homogenates—S. purpuratus homogenates (25%) were prepared as described previously (16) and stored as 0.5-ml aliquots at −80 °C. The homogenates were prepared and stored in a buffer containing 250 mM potassium gluconate, 250 mM *N*-methylglucamine, 20 mM Hepes, 1 mM $MgCl_2$, 2 units/ml creatine kinase, 4 mM creatine phosphate, and 0.5 mM ATP, pH 7.2.

Synthesis of [^{32}P-5N$_3$]NAADP—A two-step procedure similar to that used previously for the generation of [^{32}P]NAADP (17) was employed to prepare [^{32}P-5N$_3$]NAADP. In the first step, [^{32}P]NAD is converted to [^{32}P]NADP using human NAD kinase. The resulting [^{32}P]NADP is converted to [^{32}P-5N$_3$]NAADP through a base-exchange reaction catalyzed by *Aplysia* ADP-ribosyl cyclase (18). [^{32}P]NAD (1 mCi) was diluted to 500 μl with 20 mM Hepes, pH 7.3, 5 mM $MgCl_2$, 2 mM ATP, 1 mM DTT, 1 unit/ml creatine kinase, and 2 mM creatine phosphate. The reaction was started by adding 2 μg of human NAD kinase and incubated for 16 h at room temperature. The [^{32}P]NADP (80–90% yield) generated was purified by AG MP-1 chromatography. The reaction was diluted to 1 ml with water and injected onto a 0.5 × 5-cm column of AG MP-1. Elution was done with a trifluoroacetic acid gradient from 0 to 150 mM over 30 min at 1 ml/min. Eluted radioactivity was monitored with a Beckman 171M radiochemical detector. [^{32}P]NADP eluted between 15 and 17 min. The AG MP-1 chromatography system has been previously described (18). The [^{32}P]NADP was converted to [^{32}P-5N$_3$]NAADP as follows. Sodium acetate, pH 6.0 (175 μl of 500 mM), and 5N$_3$-nicotinic acid (200 μl of 500 mM in dimethyl sulfoxide) were added to 3.5 ml of purified [^{32}P]NADP. The 5N$_3$-nicotinic acid precipitates under these conditions. The pH of the sample was raised by titration with 2 M Tris base until the precipitate dissolved (~75 μl). Sodium acetate, pH 3.7 (300 μl of 500 mM) was added to readjust the pH of the sample as close to pH 4.0 as possible. The base-exchange reaction was started by adding 4 μl of 100 μg/ml *Aplysia* ADP-ribosyl cyclase and incubated at room temperature for 60–120 min. The reaction was neutralized by adding 80 μl of 2 M Tris base and was purified by AG MP-1 chromatography as described above (1.1 ml of reaction/run). The [^{32}P-5N$_3$]-NAADP eluted at 22 min and was stored unneutralized at −20 °C in 0.5-ml aliquots. It was assumed that the specific activity of the [^{32}P-5N$_3$]NAADP was the same as the commercial [^{32}P]NAD used as the starting material.

Photoaffinity Labeling of Egg Homogenates with [^{32}P-5N$_3$]-NAADP—S. purpuratus egg homogenates were diluted 10-fold with a buffer containing 250 mM potassium gluconate, 250 mM *N*-methylglucamine, 1 mM $MgCl_2$, 20 mM Hepes, pH 7.2 (KGlu buffer). The standard photolabeling protocol was as follows. The diluted homogenates (90 μl, 120 μg of protein) were incubated in a total volume of 100 μl with 2–8 nM [^{32}P-5N$_3$]NAADP for 90 min at 4 °C. Unlabeled competitors were made up to the final concentrations indicated in the figure legends. UV photolysis was accomplished by placing the samples on a sheet of Saran Wrap stretched over a block of ice and irradiated with UV light (1015 quanta/s) for 2 min in a Rayonet photochemical reactor (Southern New England Ultraviolet Co.). After photolysis, the samples were recovered and placed in microcentrifuge tubes containing 1 ml of 20 mM Hepes, pH 7.3. The samples were centrifuged at 21,000 × *g* for 10 min, and the supernatant was discarded. The membrane pellets were resuspended in 50 μl of 1× Laemmli SDS-sample buffer and subjected to SDS-polyacrylamide gel electrophoresis using 12.5% Criterion acrylamide gels. The gels were stained with SimplyBlue SafeStain, destained, and air-dried between two sheets of cellophane. Analysis of photolabeling was accomplished by exposing the dried gels to MP storage phosphor screens (Packard Instruments) for 24–120 h. The phosphor screens were developed using a Cyclone storage phosphor system (Packard Instruments). Quantification of the phosphor images was performed with the OptiQuant software (Version3.0, Packard Instruments). Because the egg homogenates were prepared and stored in the presence of 0.5 mM ATP, the standard photolabeling conditions contain 50 μM ATP.

HPLC Purification of NADP—The NADP used in competition experiments for these studies was purified immediately prior to use because NAADP was originally discovered as a contaminant in commercial NADP (19, 20). The HPLC system consisted of Beckman 125 pumps and a 166 UV detector controlled by the Nouveau Gold software and a MonoQ HR 5/5 column. The column was preconditioned with 10 mM K_2HPO_4, pH 8.0, at a flow rate of 0.5 ml/min. NADP (50 μl of 90 mM) was injected, and elution was controlled through a linear gradient (2–25 min) starting with 10 mM K_2HPO_4, pH 8.0, and ending with 50 mM K_2HPO_4, 200 mM NaCl, pH 8.0.

TPC Immunoprecipitation and Immunoblot Procedures—The antibodies to *S. purpuratus* TPCs and their coupling to protein A agarose beads have been previously described (12). For TPC immunoprecipitation studies, egg homogenate was photolabeled with [^{32}P-5N$_3$]NAADP under standard conditions (see above). Twelve samples (120 μg/sample) were combined and processed. The resulting photolabeled pellet was reconstituted in 400 μl of KGlu buffer + 1% CHAPS + Complete protease inhibitors and allowed to incubate on ice for 1.5 h. The CHAPS solubilized supernatant was obtained by centrifugation at 21,000 $\times$ *g* for 15 min. Agarose beads (100 μl) coupled to antibodies were prewashed two times with 1 ml of KGlu buffer +1% CHAPS before use. Immunoprecipitation was initiated by incubating 90 μl of photolabeled CHAPS solubilized sample with 50 μl of prewashed agarose beads coupled to control antisera or antibodies to sea urchin TPC1, TPC2, or TPC3. The samples were incubated at 4 °C for 16 h on a rotator. The samples were centrifuged at 5000 $\times$ *g* for 5 min and washed four times with 1 ml of KGlu buffer + 1% CHAPS. The samples were vigorously vortexed at each wash step, and the beads were isolated by centrifuging at 5000 $\times$ *g* for 5 min, except for the final wash in which the samples were centrifuged at 10,000 $\times$ *g* for 10 min. After the final wash, the agarose beads were suspended in 50 μl of 1$\times$ Laemmli sample buffer and incubated for 2 h at room temperature with occasional mixing. The beads were then centrifuged at 21,000 $\times$ *g* for 10 min, and the supernatants were subjected to electrophoresis on 12.5% Criterion gels as described above.

To control for any changes in protein migration caused by UV or photocross-linking, samples for immunoblot analyses were photolabeled with 1 μM 5N$_3$-NAADP, processed as above, run on 12.5% Criterion gels, and transferred to PVDF membrane for immunoblotting. A sample photolyzed with [^{32}P-5N$_3$]NAADP was included so that the positions of the photolabeled proteins could be compared with any immunoreactivity detected. The PVDF membrane was cut and subjected to Western analyses using antibodies to sea urchin TPC1, TPC2, and TPC3. Detection was by chemiluminescence using ECL reagents.

[^{32}P-5N$_3$]NAADP and [^{32}P]NAADP Binding Studies—The binding studies using [^{32}P-5N$_3$]NAADP or [^{32}P]NAADP were conducted as described previously (15).

Data Analyses—GraphPad Prism (GraphPad Software) was used for curve fitting and statistical analyses. *Error bars* shown in Figs. 3–5 represent mean ± S.E.

RESULTS AND DISCUSSION

Synthesis and Characterization of Novel NAADP-based Photoaffinity Probe—A study examining the structure-activity relationship of NAADP analogs substituted at the 4- or 5-position of nicotinic acid (15) revealed that 5N$_3$-NAADP was an agonist of calcium release from sea urchin homogenates (EC$_{50}$ of 1.7 μM) that also competed with [^{32}P]NAADP with high potency (IC$_{50}$ = 18 nM) in a competition binding assay. Such properties suggested that 5N$_3$-NAADP could prove useful as a photoaffinity probe for labeling NAADP-binding proteins. Therefore, we prepared high specific activity [^{32}P-5N$_3$]NAADP via a base-exchange reaction by incubating high specific activity

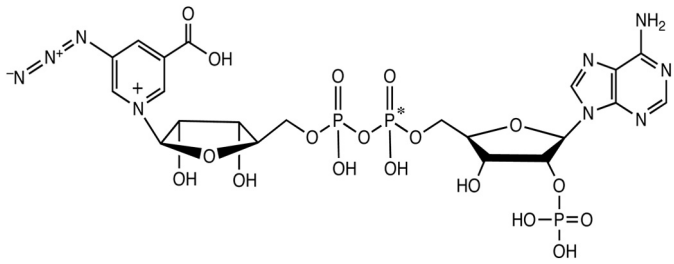

FIGURE 1. **Structure of 5-azido-NAADP.** The * denotes the phosphorus labeled with ^{32}P.

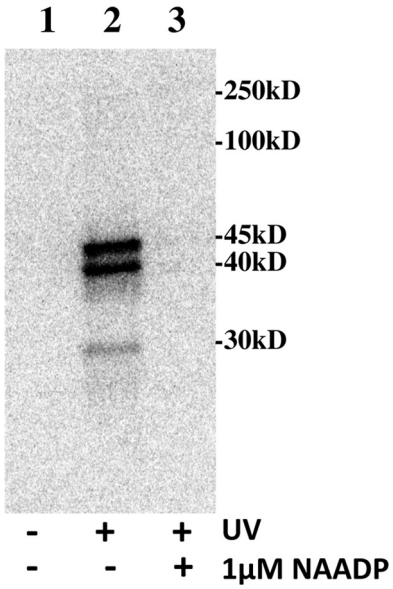

FIGURE 2. **[^{32}P-5N$_3$]NAADP photoaffinity labeling is UV-dependent and blocked by unlabeled NAADP.** *S. purpuratus* egg homogenates were incubated with [^{32}P-5N$_3$]NAADP for 90 min in the absence (*lanes 1* and *2*) or presence (*lane 3*) of 1 μM NAADP. *Lane 1* represents a control that was not subjected to UV light. *Lanes 2* and *3* were subjected to UV light. Image is a phosphor image of the resulting gel (see "Experimental Procedures" for standard conditions).

[^{32}P]NADP with 5-azido-nicotinic acid and *Aplysia* ADP-ribosyl cyclase (18) to yield [^{32}P-5N$_3$]NAADP (structure shown in Fig. 1).

The ability of the [^{32}P-5N$_3$]NAADP probe to detect high affinity NAADP-binding proteins was assessed in Fig. 2. *S. purpuratus* egg homogenates were incubated for 90 min with [^{32}P-5N$_3$]NAADP in the absence or presence of 1 μM unlabeled NAADP, and then the effect of UV exposure was examined. No proteins were labeled if the sample was not subjected to UV light to activate the probe (Fig. 2, *lane 1*). However, several proteins were labeled (45, 40, and 30 kDa) when the sample was exposed to UV (Fig. 2, *lane 2*). The 45- and 40-kDa proteins labeled to approximately the same extent, with the 30-kDa protein accounting for 10% of the total specific labeling. Inclusion of unlabeled 1 μM NAADP in the incubation prevented the labeling of the 45-, 40-, and 30-kDa proteins (Fig. 2, *lane 3*). These data confirm that the [^{32}P-5N$_3$]NAADP probe is UV-sensitive and that an excess of unlabeled NAADP protects the labeling of the proteins. Furthermore, the time courses for [^{32}P-5N$_3$]NAADP photolabeling of the 45-, 40-, and 30-kDa proteins and [^{32}P-5N$_3$]NAADP binding were similar, and both maximized between 60 and 100 min (supplemental Fig. 1S).

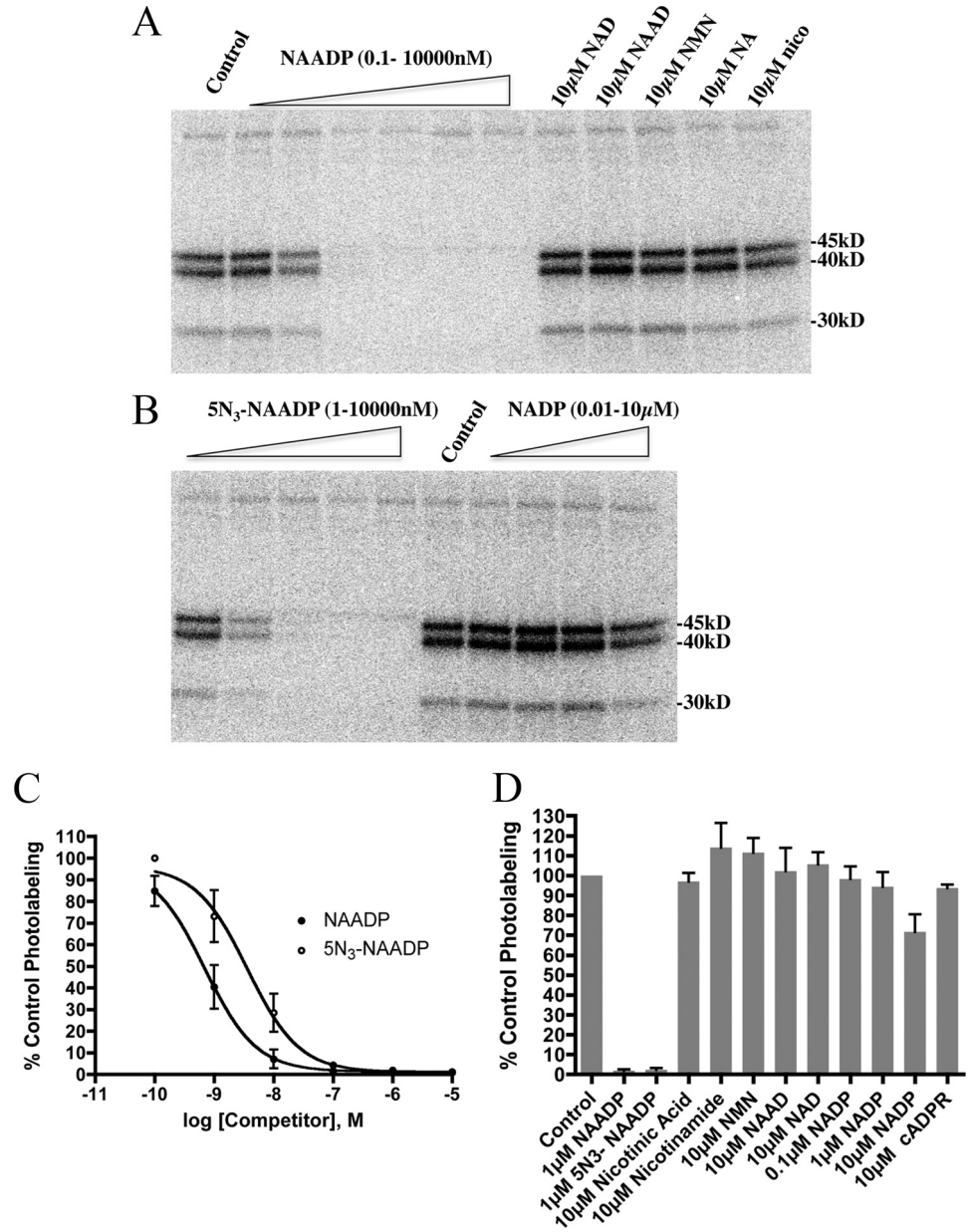

FIGURE 3. **Specificity of [^{32}P-5N$_3$]NAADP photolabeling in sea urchin egg homogenates.** Photolabeling was performed in the absence or presence of the indicated concentrations of various competitors. *A*, phosphor image of a gel examining the effect of NAADP, NAD, NAAD, nicotinamide mononucleotide (*NMN*), nicotinic acid (*NA*), and nicotinamide (*nico*). The concentrations of NAADP range from 0.1 to 10,000 nM in 10-fold increments. *B*, phosphor image of a gel examining the effect of 5N$_3$-NAADP and NADP. The concentration of unlabeled 5N$_3$-NAADP ranges from 1 to 10,000 nM in 10-fold increments. *C*, competition of [^{32}P-5N$_3$]NAADP photolabeling (45-, 40-, and 30-kDa bands combined) by unlabeled NAADP and 5N$_3$-NAADP. Data represent the mean ± S.E. ($n = 4$) of densitometric analyses of experiments similar to those shown in *panels A* and *B*. *D*, the effect of various nucleotides on [^{32}P-5N$_3$]NAADP photolabeling (45-, 40-, and 30-kDa bands). Data represent the mean ± S.E. ($n = 4$) of densitometric analyses of experiments similar to those shown in *panels A* and *B*. *cADPR*, cyclic ADP-ribose.

This pattern of [^{32}P-5N$_3$]NAADP photolabeling was consistent between 32 different *S. purpuratus* egg homogenate preparations, and the extent of [^{32}P]NAADP binding correlated with the intensity of photolabeling (supplemental Fig. 2S). Preparations with low NAADP binding activity did not photolabel efficiently.

Specificity of [^{32}P-5N$_3$]NAADP Photolabeling—How specific was the photoaffinity labeling of the 45-, 40-, and 30-kDa proteins by [^{32}P-5N$_3$]NAADP? Inclusion of unlabeled NAADP (Fig. 3*A*) or 5N$_3$-NAADP (Fig. 3*B*) reduced the labeling of the 45-, 40-, and 30-kDa proteins in a concentration-dependent manner. Half-maximal reduction of the photolabeling of these bands occurred at ~0.7 nM NAADP and 4 nM 5N$_3$-NAADP (Fig. 3*C*). The competition kinetics were similar for all three labeled proteins. Structurally related nucleotides such as NAD, NAAD, nicotinamide mononucleotide, nicotinic acid, and nicotinamide did not affect the ability of [^{32}P-5N$_3$]NAADP to photolabel the 45-, 40-, and 30-kDa proteins even at concentrations as high as 10 μM (Fig. 3, *A* and *D*). NADP did reduce the photolabeling of these bands by about 30% at 10 μM (Fig. 3, *B* and *D*), although the NADP was purified by HPLC immediately prior to the experiment to remove contaminating NAADP. The

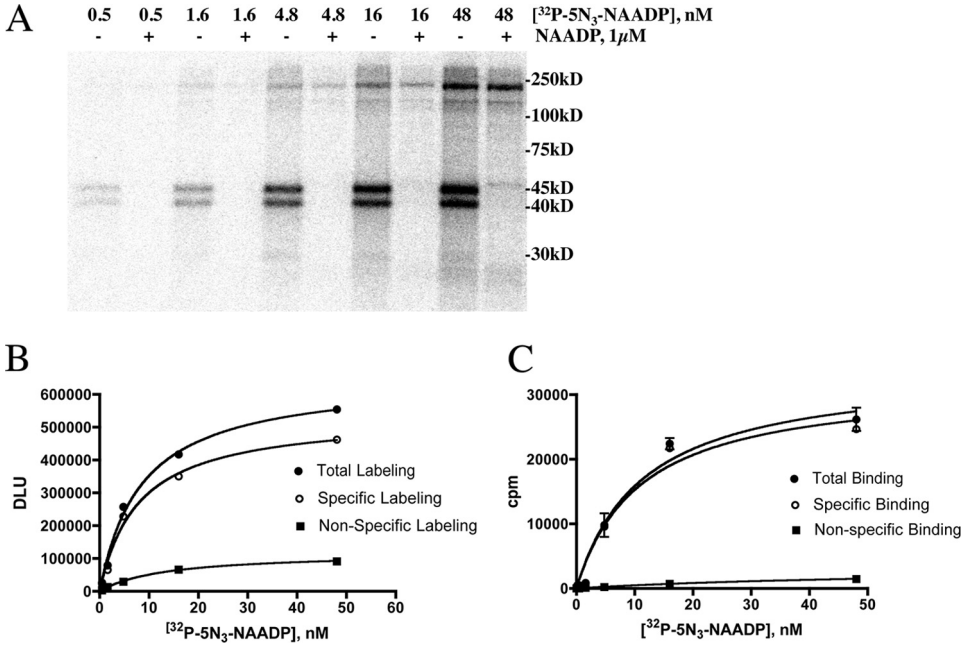

FIGURE 4. **[^{32}P-5N$_3$]NAADP photolabeling and binding display saturable kinetics.** *A*, photolabeling of sea urchin egg homogenate performed at increasing concentrations of [^{32}P-5N$_3$]NAADP in the absence (−) or presence of (+) 1 μM NAADP. A phosphor image of acrylamide gel is shown. *B*, saturation kinetics of [^{32}P-5N$_3$]NAADP photolabeling. Total labeling (*closed circles*), nonspecific labeling (in the presence of 1 μM NAADP, *closed squares*), and specific labeling (*open circles*) were determined from densitometric analyses of phosphor images of experiments similar to the one shown in *panel A* ($n = 3$). *DLU*, digital light units. *C*, saturation kinetics of [^{32}P-5N$_3$]NAADP binding. The conditions for binding were the same as used for photoaffinity labeling. Total binding (*closed circles*), nonspecific binding (in the presence of 1 μM NAADP, *closed squares*), and specific binding (*open circles*) were determined by a conventional filtration binding assay.

specificity of [^{32}P-5N$_3$]NAADP photolabeling shown in Fig. 3 is similar to the specificity of [^{32}P]NAADP binding previously observed in this system (17, 21) and consistent with photolabeling data observed in another sea urchin species (22).

Fig. 4 shows the dependence of [^{32}P-5N$_3$]NAADP photolabeling and binding on the concentration of [^{32}P-5N$_3$]NAADP. Fig. 4*A* shows that the intensity of the labeling of the 45-, 40-, and 30-kDa proteins and others, most notably proteins between 100 and 250 kDa, increased as the concentration of labeled photoprobe is increased. Only the 45-, 40-, and 30-kDa proteins were labeled specifically as inclusion of unlabeled 1 μM NAADP prevented the labeling of these proteins but not the others. Fig. 4, *B* and *C*, compare saturation kinetics of [^{32}P-5N$_3$]NAADP photolabeling with [^{32}P-5N$_3$]NAADP binding kinetics determined by a conventional filtration binding assay. Nonspecific binding was estimated in both experiments by determining the photolabeling or binding in the presence of 1 μM NAADP at each concentration of [^{32}P-5N$_3$]NAADP. Specific photolabeling was determined by densitometry analyses of the data shown in Fig. 4*A* (specific photolabeling is the difference between the labeling in the absence and presence of 1 μM NAADP). Both photolabeling and binding appear to saturate as the concentration of [^{32}P-5N$_3$]NAADP approaches 50 nM. The K_d values calculated from non-linear regression analysis of the specific labeling and binding data curves in Fig. 4, *B* and *C*, are comparable (8 and 11 nM for photolabeling and binding, respectively). The data in Fig. 4 demonstrate that the [^{32}P-5N$_3$]NAADP probe can detect high affinity NAADP binding sites by both photocrosslinking and conventional binding assays.

Perhaps the most novel feature of the NAADP system in sea urchin eggs, but not mammalian systems, is a self-inactivation process by which the NAADP-induced calcium release can be totally inactivated by very low, subthreshold concentrations of NAADP (17, 23). The self-inactivation process is time- and concentration-dependent. Full inactivation is observed with as low as 1 nM NAADP in 10 min (the threshold NAADP concentration for calcium release is about 10 nM) (17, 23). This self-inactivation process occurs at the receptor level, as we have shown that preincubation of microsomes with subthreshold concentrations of [^{32}P]NAADP (1–2 nM) prevents higher concentrations of unlabeled NAADP from competing with the labeled NAADP in a time-dependent manner (17). It appears that binding of subthreshold concentrations of NAADP induces a change in the receptor that results in the inability of the bound NAADP to exchange with free NAADP (17). The self-inactivation has also been shown to occur in intact eggs by microinjecting either NAADP (23) or caged NAADP (17). The apparent irreversibility of binding has been shown to be a consequence of the high K^+ concentrations present in the preparation (17, 21, 24). This feature does not occur in the presence of Na^+ ions or at lower concentrations of K^+ (24). We assessed whether a similar phenomenon occurs with [^{32}P-5N$_3$]NAADP photoaffinity labeling. *S. purpuratus* egg homogenate was preincubated with 1 nM [^{32}P-5N$_3$]NAADP in either a high (250 mM) or a low K^+ (25 mM) buffer, and unlabeled 500 nM NAADP was added at 0, 2, 5, 15 or 30 min. Ninety minutes after initiating the reaction with label, the samples were photoaffinity-labeled by exposing to UV light. Fig. 5*A* shows that unlabeled NAADP is unable to completely protect photolabeling if added at various times after starting the preincubation with [^{32}P-5N$_3$]NAADP when conducted in the presence of 250 mM K^+. Complete protection of photolabeling only occurs if the unla-

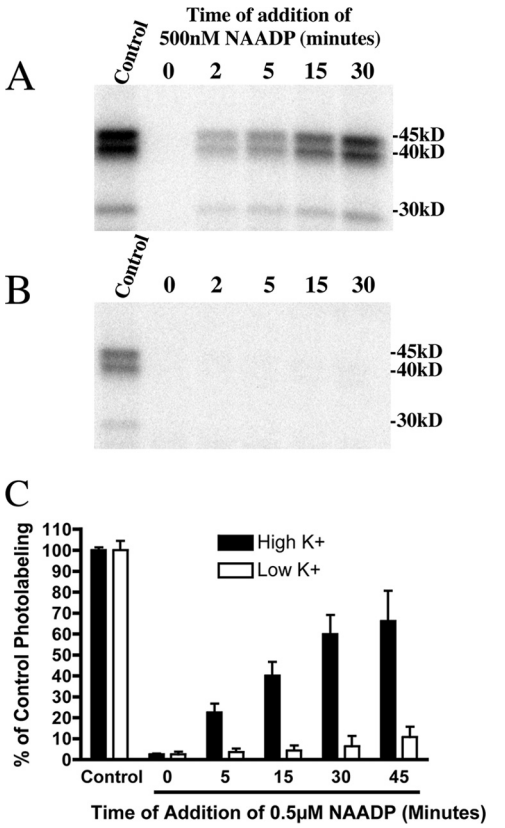

FIGURE 5. **[^{32}P-5N$_3$]NAADP photolabeling displays apparent irreversibility in high K$^+$.** *A* and *B*, *S. purpuratus* egg homogenates were incubated with 1 nM [^{32}P-5N$_3$]NAADP for 90 min in either high K$^+$ (250 mM, *A*) or low K$^+$ (25 mM, *B*). Unlabeled 500 nM NAADP was added to the incubation at 0, 2, 5, 15, and 30 min. All samples were photolabeled after 90 min in the presence of [^{32}P-5N$_3$]NAADP. Control samples were incubated with [^{32}P-5N$_3$]NAADP only. Phosphor images of the acrylamide gels are shown. *C*, densitometric analyses of experiments similar to those shown in *panels A* and *B* ($n = 4$).

beled NAADP and [^{32}P-5N$_3$]NAADP are added together (addition at 0 min). However, if the unlabeled NAADP is added 30 min after the label, ~60% of control photolabeling remains (Fig. 5, *A* and *C*). The magnitude of photolabeling protection is dependent on the time of preincubation with the label, with less protection the longer the [^{32}P-5N$_3$]NAADP was allowed to incubate with homogenate before the addition of the unlabeled NAADP. Fig. 5*B* demonstrates that adding unlabeled NAADP at various times after starting the preincubation with [^{32}P-5N$_3$]NAADP does protect the photolabeling when conducted in the presence of a low K$^+$ (25 mM) buffer, suggesting that the unlabeled NAADP is able to compete with the [^{32}P-5N$_3$]NAADP under these conditions. Fig. 5*C* provides a quantitative summary of these experiments. These data indicate that the proteins detected by [^{32}P-5N$_3$]NAADP photoaffinity labeling in the sea urchin egg system possess the property of apparent irreversibility in high K$^+$ similar to that previously described for the high affinity NAADP binding (17, 21, 24).

TPCs have recently been shown to be activated by NAADP (4–6) (see Refs. 25–30 for recent reviews). Notably, the sea urchin TPCs have monomeric sizes ranging from 75 to 94 kDa, which is larger than the proteins detected by the [^{32}P-5N$_3$]NAADP photoprobe. To examine the relationship between TPCs and the proteins specifically photolabeled by

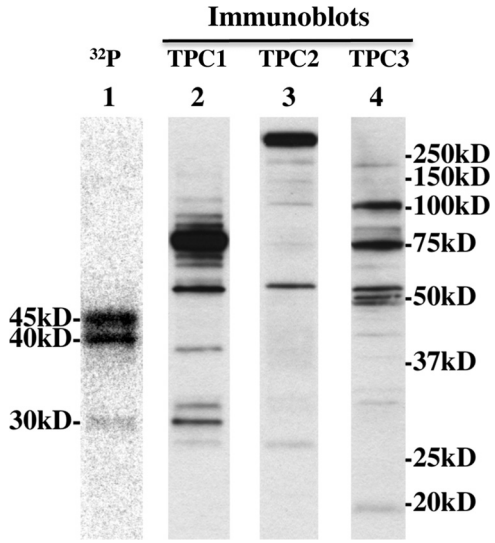

FIGURE 6. **TPC immunoblot analyses of egg homogenates.** *S. purpuratus* egg homogenates photolabeled in the presence of 1 μM unlabeled 5N$_3$-NAADP were subjected to immunoblotting as described under "Experimental Procedures" using affinity-purified antibodies against TPC1 (*lane 2*), TPC2 (*lane 3*), and TPC3 (*lane 4*). *Lane 1* is a phosphor image of the same egg homogenate photolabeled with [^{32}P-5N$_3$]NAADP under standard conditions.

[^{32}P-5N$_3$]NAADP, we compared [^{32}P-5N$_3$]NAADP photolabeling with TPC immunoreactivity. Fig. 6 (*lanes 2–4*) shows immunoblots of *S. purpuratus* egg extracts probed with affinity-purified antibodies to sea urchin TPC1, TPC2, and TPC3. The egg homogenates subjected to immunoblotting were photoaffinity-labeled with 1 μM unlabeled 5N$_3$-NAADP to control for any changes in protein migration on the gel caused by cross-linking or UV exposure. The same egg extract photoaffinity-labeled with [^{32}P-5N$_3$]NAADP under standard conditions was run on the same gel for comparison (Fig. 6, *lane 1*). The immunoblot was overexposed on purpose to expose any immunoreactivity in the molecular mass region (30–45 kDa) where specific photolabeling occurs. As shown in Fig. 6, the antibody to TPC1 detects a major band at ~75 kDa, the antibody against TPC2 detects heavy immunoreactivity in the >250-kDa region (likely representing TPC2 dimers or multimers (31), and the antibody against TPC3 detected several proteins with the major immunoreactivity at ~75 and 100 kDa. In each case, the photolabeled proteins migrate at a much smaller size than the corresponding TPC isoform, and the predominant 45- and 40-kDa photolabeled proteins (implicated by immunoprecipitation, see below) do not align with TPC immunoreactivity. These data argue against the [^{32}P-5N$_3$]NAADP photolabeled proteins being TPCs or TPC degradation products.

Ruas *et al.* (12), employing an immunoprecipitation strategy, recently demonstrated that antibodies against sea urchin TPCs were able to immunoprecipitate NAADP binding activity. In these experiments, [^{32}P]NAADP binding was found in anti-TPC1, anti-TPC2 (although at low levels), and anti-TPC3 immunoprecipitates (12). The NAADP binding found in the immunoprecipitates displayed the hallmark features of the high affinity NAADP receptor in terms of affinity, specificity, and irreversibility in high K$^+$ buffer (12), similar to the findings reported here (Figs. 3–5) for [^{32}P-5N$_3$]NAADP photoaffinity labeling. We conducted similar immunoprecipitation exper-

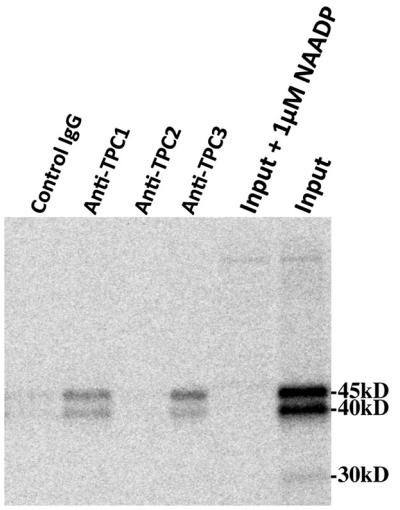

FIGURE 7. **Antibodies to sea urchin TPC1and TPC3 specifically immunoprecipitate proteins photoaffinity-labeled with [^{32}P-5N$_3$]NAADP.** The *first four lanes* (*left* to *right*) are immunoprecipitated fractions from experiments using control antibody-, anti-TPC1-, anti-TPC2-, and anti-TPC3-coupled agarose beads, respectively. The *far right lane* (*Input lane*) is the input extract used for the immunoprecipitation experiments and represents CHAPS solubilized egg extract photolabeled in the absence 5 μM NAADP. The lane labeled *Input + 1μM NAADP* represents CHAPS-solubilized egg extract photolabeled in the absence of 5 μM NAADP. A phosphor image of the gel is shown.

iments using affinity-purified antibodies to sea urchin egg TPCs that were coupled to protein A-agarose beads. Sea urchin egg homogenates were photoaffinity-labeled with [^{32}P-5N$_3$]NAADP, and the membranes were solubilized with CHAPS after the removal of free label. The CHAPS-solubilized photoaffinity-labeled preparation (Fig. 7, *Input lane*) was then subjected to the immunoprecipitation protocol using agarose beads coupled to control antibody and antibodies to each of the three sea urchin TPCs (see "Experimental Procedures"). Fig. 7 shows the result of a typical experiment. Both anti-TPC1 and anti-TPC3 beads, but not control or anti-TPC2 beads (*lanes 1* and *3*), were able to immunoprecipitate 45- and 40-kDa photolabeled proteins. Approximately 5% of the total photolabeled material binds to the anti-TPC1 and anti-TPC3 beads. The input for this experiment is shown in Fig. 7, *far right lane*. It appears that the TPC1 and TPC3 immunoprecipitates contain more of the 45-kDa protein band than the 40-kDa protein. No 30-kDa protein was detected in these immunoprecipitates. Overall, the ability of anti-TPC1 and anti-TPC3 beads to pull down a portion of the specifically photolabeled proteins indicates that these proteins likely form a complex with TPCs. Ruas *et al.* (12) postulated a similar conjecture using an immunoprecipitation strategy. Although not described in their study, about 3% of total binding activity of the input extract was immunoprecipitated by anti-TPC1 and anti-TPC3 beads,[4] similar to the amount of photolabel immunoprecipitated in our experiments. The TPC immunoprecipitation data strongly indicate that high affinity NAADP-binding proteins (whether assessed by binding or photoaffinity labeling) form complexes with TPCs.

The suggestion that high affinity NAADP-binding proteins are distinct but associate with TPCs is not inconsistent with previous observations. When mammalian TPC2 was overexpressed, a 3-fold increase in NAADP binding occurred despite a large (>250-fold) increase in TPC2 mRNA (4). This small increase in binding could be a compensatory change due to a large change in an associated protein. Furthermore, the immunoprecipitation studies reported here and those of Ruas *et al.* (12) are more consistent with NAADP-binding proteins forming a complex with TPCs than with TPCs directly binding NAADP based on the amount of photolabeled protein or NAADP binding present in the immunocomplexes.

In the companion study, Lin-Moshier *et al.* (22) employed a similar strategy to investigate NAADP-binding proteins in mammalian systems and show similar findings. [^{32}P-5N$_3$]NAADP specifically photolabeled proteins in multiple mammalian systems that were smaller than the TPCs. Overexpression or ablation of mammalian TPCs did not change the photoaffinity labeling pattern, nor was label associated with endogenous or exogenously expressed TPCs (22). It is also notable that the apparent size of the two high affinity mammalian proteins (22/23 kDa) was lower than the candidate implicated in the sea urchin species (45/40 kDa, 41 kDa in Ref. 22). This observation is not surprising given the different characteristics of NAADP-evoked Ca^{2+} release in urchin and mammalian systems, and identification of these different candidates will be required to establish their interrelationship.

In conclusion, we have synthesized and characterized [^{32}P-5N$_3$]NAADP as a photoaffinity probe for NAADP-binding proteins. This reagent will be a useful probe in the identification of NAADP-binding proteins, especially when combined with mass spectrometry (14). Using sea urchin egg homogenates, [^{32}P-5N$_3$]NAADP was found to photolabel several proteins that possessed properties similar to the high affinity NAADP binding previously studied in this system (17, 21). The photolabeled proteins were smaller than TPCs, but immunoprecipitation studies suggested that the photolabeled proteins associated with sea urchin TPC1 and TPC3. These data suggest that a larger NAADP-sensitive complex containing the TPC channel is responsible for mediating NAADP-evoked calcium release.

[4] M. Ruas and A. Galione, personal communication.

REFERENCES

1. Galione, A., Morgan, A. J., Arredouani, A., Davis, L. C., Rietdorf, K., Ruas, M., and Parrington, J. (2010) NAADP as an intracellular messenger regulating lysosomal calcium-release channels. *Biochem. Soc. Trans* **38,** 1424–1431
2. Lee, H. C. (2005) Nicotinic acid adenine dinucleotide phosphate (NAADP)-mediated calcium signaling. *J. Biol. Chem.* **280,** 33693–33696
3. Guse, A. H., and Lee, H. C. (2008) NAADP: a universal Ca^{2+} trigger. *Sci. Signal.* **1,** re10
4. Calcraft, P. J., Ruas, M., Pan, Z., Cheng, X., Arredouani, A., Hao, X., Tang, J., Rietdorf, K., Teboul, L., Chuang, K. T., Lin, P., Xiao, R., Wang, C., Zhu, Y., Lin, Y., Wyatt, C. N., Parrington, J., Ma, J., Evans, A. M., Galione, A., and Zhu, M. X. (2009) NAADP mobilizes calcium from acidic organelles through two-pore channels. *Nature* **459,** 596–600
5. Brailoiu, E., Churamani, D., Cai, X., Schrlau, M. G., Brailoiu, G. C., Gao, X., Hooper, R., Boulware, M. J., Dun, N. J., Marchant, J. S., and Patel, S. (2009) Essential requirement for two-pore channel 1 in NAADP-mediated calcium signaling. *J. Cell Biol.* **186,** 201–209
6. Zong, X., Schieder, M., Cuny, H., Fenske, S., Gruner, C., Rötzer, K., Griesbeck, O., Harz, H., Biel, M., and Wahl-Schott, C. (2009) The two-pore channel TPCN2 mediates NAADP-dependent Ca^{2+} release from lysosomal stores. *Pflugers Arch* **458,** 891–899

7. Brailoiu, E., Hooper, R., Cai, X., Brailoiu, G. C., Keebler, M. V., Dun, N. J., Marchant, J. S., and Patel, S. (2010) An ancestral deuterostome family of two-pore channels mediates nicotinic acid adenine dinucleotide phosphate-dependent calcium release from acidic organelles. *J. Biol. Chem.* **285,** 2897–2901
8. Brailoiu, E., Rahman, T., Churamani, D., Prole, D. L., Brailoiu, G. C., Hooper, R., Taylor, C. W., and Patel, S. (2010) An NAADP-gated two-pore channel targeted to the plasma membrane uncouples triggering from amplifying Ca^{2+} signals. *J. Biol. Chem.* **285,** 38511–38516
9. Pitt, S. J., Funnell, T. M., Sitsapesan, M., Venturi, E., Rietdorf, K., Ruas, M., Ganesan, A., Gosain, R., Churchill, G. C., Zhu, M. X., Parrington, J., Galione, A., and Sitsapesan, R. (2010) TPC2 is a novel NAADP-sensitive Ca^{2+} release channel, operating as a dual sensor of luminal pH and Ca^{2+}. *J. Biol. Chem.* **285,** 35039–35046
10. Schieder, M., Rötzer, K., Brüggemann, A., Biel, M., and Wahl-Schott, C. A. (2010) Characterization of two-pore channel 2 (TPCN2)-mediated Ca^{2+} currents in isolated lysosomes. *J. Biol. Chem.* **285,** 21219–21222
11. Yamaguchi, S., Jha, A., Li, Q., Soyombo, A. A., Dickinson, G. D., Churamani, D., Brailoiu, E., Patel, S., and Muallem, S. (2011) Transient receptor potential mucolipin 1 (TRPML1) and two-pore channels are functionally independent organellar ion channels. *J. Biol. Chem.* **286,** 22934–22942
12. Ruas, M., Rietdorf, K., Arredouani, A., Davis, L. C., Lloyd-Evans, E., Koegel, H., Funnell, T. M., Morgan, A. J., Ward, J. A., Watanabe, K., Cheng, X., Churchill, G. C., Zhu, M. X., Platt, F. M., Wessel, G. M., Parrington, J., and Galione, A. (2010) Purified TPC isoforms form NAADP receptors with distinct roles for Ca^{2+} signaling and endolysosomal trafficking. *Curr. Biol.* **20,** 703–709
13. Dormán, G., and Prestwich, G. D. (2000) Using photolabile ligands in drug discovery and development. *Trends Biotechnol.* **18,** 64–77
14. Robinette, D., Neamati, N., Tomer, K. B., and Borchers, C. H. (2006) Photoaffinity labeling combined with mass spectrometric approaches as a tool for structural proteomics. *Expert Rev. Proteomics* **3,** 399–408
15. Jain, P., Slama, J. T., Perez-Haddock, L. A., and Walseth, T. F. (2010) Nicotinic acid adenine dinucleotide phosphate analogues containing substituted nicotinic acid: effect of modification on Ca^{2+} release. *J. Med. Chem.* **53,** 7599–7612
16. Lee, H. C., Aarhus, R., Gee, K. R., and Kestner, T. (1997) Caged nicotinic acid adenine dinucleotide phosphate. Synthesis and use. *J. Biol. Chem.* **272,** 4172–4178
17. Aarhus, R., Dickey, D. M., Graeff, R. M., Gee, K. R., Walseth, T. F., and Lee, H. C. (1996) Activation and inactivation of Ca^{2+} release by $NAADP^+$. *J. Biol. Chem.* **271,** 8513–8516
18. Aarhus, R., Graeff, R. M., Dickey, D. M., Walseth, T. F., and Lee, H. C. (1995) ADP-ribosyl cyclase and CD38 catalyze the synthesis of a calcium-mobilizing metabolite from NADP. *J. Biol. Chem.* **270,** 30327–30333
19. Clapper, D. L., Walseth, T. F., Dargie, P. J., and Lee, H. C. (1987) Pyridine nucleotide metabolites stimulate calcium release from sea urchin egg microsomes desensitized to inositol trisphosphate. *J. Biol. Chem.* **262,** 9561–9568
20. Lee, H. C., and Aarhus, R. (1995) A derivative of NADP mobilizes calcium stores insensitive to inositol trisphosphate and cyclic ADP-ribose. *J. Biol. Chem.* **270,** 2152–2157
21. Billington, R. A., and Genazzani, A. A. (2000) Characterization of $NAADP^+$ binding in sea urchin eggs. *Biochem. Biophys. Res. Commun.* **276,** 112–116
22. Lin-Moshier, Y., Walseth, T. F., Churamani, D., Slama, J. T., Hooper, R., Brailoiu, G. C., Patel, S., and Marchant, J. S. (2012) Photoaffinity labeling of nicotinic acid adenine dinucleotide phosphate (NAADP) targets in mammalian cells. *J. Biol. Chem.* **278,** 2296–2307
23. Genazzani, A. A., Empson, R. M., and Galione, A. (1996) Unique inactivation properties of NAADP-sensitive Ca^{2+} release. *J. Biol. Chem.* **271,** 11599–11602
24. Dickinson, G. D., and Patel, S. (2003) Modulation of NAADP (nicotinic acid-adenine dinucleotide phosphate) receptors by K^+ ions: evidence for multiple NAADP receptor conformations. *Biochem. J.* **375,** 805–812
25. Zhu, M. X., Ma, J., Parrington, J., Galione, A., and Evans, A. M. (2010) TPCs: endolysosomal channels for Ca^{2+} mobilization from acidic organelles triggered by NAADP. *FEBS Lett.* **584,** 1966–1974
26. Zhu, M. X., Ma, J., Parrington, J., Calcraft, P. J., Galione, A., and Evans, A. M. (2010) Calcium signaling via two-pore channels: local or global, that is the question. *Am. J. Physiol. Cell Physiol.* **298,** C430–C441
27. Zhu, M. X., Evans, A. M., Ma, J., Parrington, J., and Galione, A. (2010) Two-pore channels for integrative Ca signaling. *Commun. Integr Biol.* **3,** 12–17
28. Patel, S., Marchant, J. S., and Brailoiu, E. (2010) Two-pore channels: regulation by NAADP and customized roles in triggering calcium signals. *Cell Calcium* **47,** 480–490
29. Evans, A. M. (2010) The role of intracellular ion channels in regulating cytoplasmic calcium in pulmonary arterial smooth muscle: which store and where? *Adv. Exp. Med. Biol.* **661,** 57–76
30. Galione, A., Evans, A. M., Ma, J., Parrington, J., Arredouani, A., Cheng, X., and Zhu, M. X. (2009) The acid test: the discovery of two-pore channels (TPCs) as NAADP-gated endolysosomal Ca^{2+} release channels. *Pflugers Arch* **458,** 869–876
31. Rietdorf, K., Funnell, T. M., Ruas, M., Heinemann, J., Parrington, J., and Galione, A. (2011) Two-pore channels form homo- and heterodimers. *J. Biol. Chem.* **286,** 37058–37062